THE JOURNAL OF PHYSICAL CHEMISTRY C
A JOURNAL OF THE AMERICAN CHEMICAL SOCIETY

pubs.acs.org/JPCC

Article

Pressure-Stimulated Photopolymerization in Fullerene Layers of a Molecular Complex $[\{Zn(Et_2dtc)\}_2 \cdot DABCO] \cdot C_{60} \cdot (DABCO)_2$

Konstantin P. Meletov,* Alexey V. Kuzmin, and Maxim A. Faraonov

Cite This: *J. Phys. Chem. C* 2024, 128, 597−604

Read Online

ACCESS | Metrics & More | Article Recommendations

ABSTRACT: The behavior of the fullerene molecular complex $[\{Zn(Et_2dtc)\}_2 \cdot DABCO] \cdot C_{60} \cdot (DABCO)_2$ at high pressure was studied by Raman spectroscopy and X-ray diffraction (XRD) using the diamond anvil cell technique. The Raman spectra taken at room temperature with a green laser of 532 nm showed a peculiarity near 2 GPa related to the formation of interfullerene covalent bonds. However, the XRD study up to 2.6 GPa showed smooth and monotonous pressure dependence of the lattice parameters and cell volume well fitted by the Murnaghan equation of state with K_0 = 10.67 GPa and K' = 6.96. The changes in the Raman spectra were caused by photoinduced polymerization in fullerene layers that could be suppressed when using a near-infrared laser of 785 nm. The photopolymerization at elevated pressure had a thermal activation character; the activation energy of 1.09 eV at 1.05 GPa decreased to 0.18 eV at 1.85 GPa, which gave rise to a fast photopolymerization at room temperature.

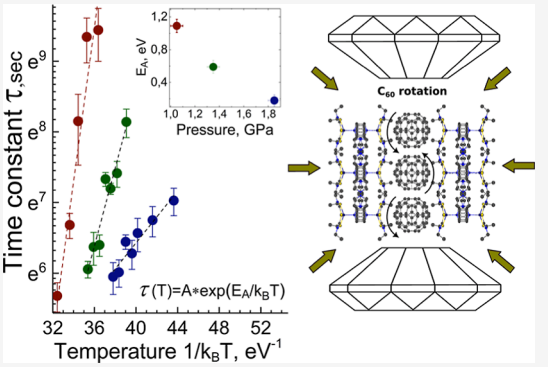

1. INTRODUCTION

The molecular complexes of C_{60} have a layered structure with a weak van der Waals intermolecular interaction, in which the close-packed molecules in the fullerene acceptor layers are alternated with layers of the molecular donor. The behavior of the fullerene complexes at high pressure is of interest due to the reduction of interfullerene and interlayer distances, resulting in an increased overlap of the molecular orbitals. The overlap of the highest occupied molecular orbital (HOMO) of the molecular donor and the lowest unoccupied molecular orbital (LUMO) of the fullerene acceptor stimulates the charge transfer between them, as well as charge redistribution on the fullerene molecule cage. In addition, a decrease in the interfullerene distances at high pressure raises the possibility of covalent bonding between adjacent fullerene molecules. The formation of covalent bonds in the fullerene layers at high pressure was reported in a number of Raman studies of various molecular complexes and doped C_{60} materials.[1−9] On the other hand, the covalent bonding of C_{60} in the fullerene layers of molecular complexes $\{Pt(dbdtc)_2\} \cdot C_{60}$ and $\{Pt(nPr_2dtc)_2\} \cdot (C_{60})_2$ was observed even at ambient conditions under laser irradiation[10,11] In fact, the photoinduced polymerization of C_{60} films under intense UV or visible light was observed for the first time much earlier.[12] Finally, photopolymerization in the fullerene layers of a $\{Cd(dedtc)_2\}_2 \cdot C_{60}$ complex was observed in the Raman spectra between 2 and 6 GPa at ambient temperature while outside this pressure range photopolymerization was suppressed.[13]

The photopolymerization of pristine C_{60} occurs in the surfaces of bulk samples owing to small light penetration depth (~1 μm near 500 nm); the phototransformed material is rather disordered and contains various oligomers.[12,14,15] The bulk fullerene polymers synthesized under high-pressure/high-temperature (HPHT) treatment of the C_{60} powder are highly ordered, and their crystalline structures have been identified by X-ray diffraction (XRD) as one-dimensional orthorhombic (1D-O), as well as two-dimensional tetragonal (2D-T) and rhombohedral (2D-R).[16,17] The polymerization of C_{60} occurs via the [2 + 2] cycloaddition mechanism that necessitates the rotation of molecules to attain a suitable mutual orientation when the double C═C bonds of adjacent molecules face each other.[18] The phonon modes of crystalline C_{60} polymers exhibit splitting and softening due to the lowering of the molecular symmetry caused by intermolecular covalent bonds.[19,20] The Raman examination of the C_{60} polymers is based mainly on the A_g (2) pentagonal pinch mode (PP-mode) behavior associated with the in-phase stretching vibration, which involves tangential displacements of carbon atoms with the contraction of the pentagonal rings and expansion of the hexagonal rings.

Received: October 23, 2023
Revised: December 13, 2023
Accepted: December 14, 2023
Published: December 28, 2023

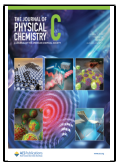

https://doi.org/10.1021/acs.jpcc.3c06997
J. Phys. Chem. C 2024, 128, 597−604

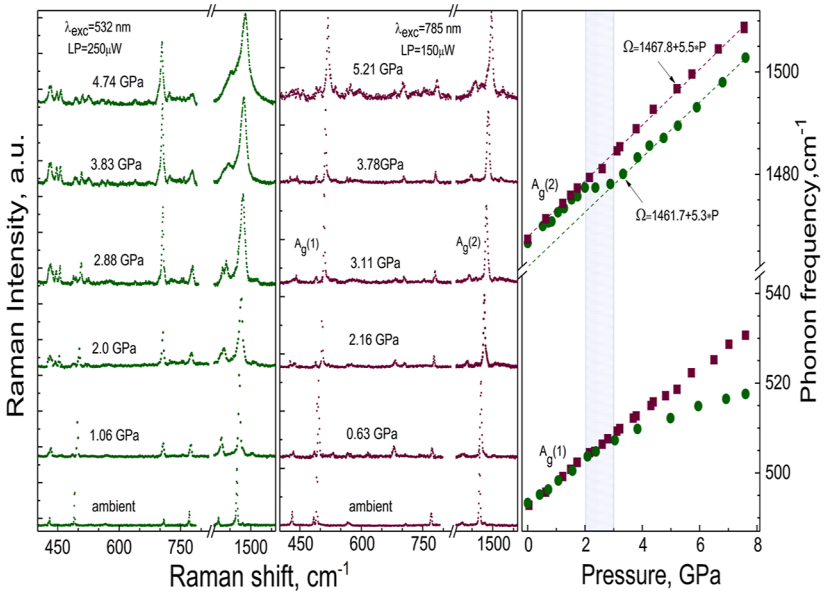

Figure 1. Raman spectra of the $[\{Zn(Et_2dtc)\}_2{\cdot}DABCO]{\cdot}C_{60}{\cdot}(DABCO)_2$ complex at high pressure recorded with λ_{exc} = 532 nm (left panel) and with λ_{exc} = 785 nm (central panel). Right panel—pressure dependence of the A_g (1) and A_g (2) mode frequencies. Circles—λ_{exc} = 532 nm, squares—λ_{exc} = 785 nm, and dotted lines—linear fits.

The PP-mode frequency downshifts due to the lowering of the average cage stiffness with the appearance and an increase in the number of the sp^3-like coordinated carbon atoms per C_{60} molecule associated with the intercage bonds. The A_g (2) mode of the C_{60} monomer at 1468 cm^{-1} shifts down to 1458 cm^{-1} in the linear chains (1D-O polymer, 4 sp^3-like coordinated carbon atoms), while in the planar polymers, the peak downshifts further to 1446 cm^{-1} (2D-T polymer, 8 sp^3-like coordinated carbon atoms) and 1408 cm^{-1} (2D-R polymer, 12 sp^3-like coordinated carbon atoms).[19−21] Furthermore, the PP-mode downshifts in fullerenes doped with alkali metals due to the lowering of the cage stiffness caused by electron transfer from a metal to a fullerene molecule, which results in PP-mode softening of about 6 cm^{-1} for every transferred electron.[22]

The ability of C_{60} to form intermolecular covalent bonds is due to the existence of 30 unsaturated double C═C bonds in the fullerene molecule cage. Usually, fullerene molecules are oriented so that the double C═C bond of one molecule faces the electron-poor center of the hexagon (H-orientation) or the center of the pentagon (P-orientation) of another molecule. The H- and P-orientations minimize the Coulombic repulsion energy and correspond to the local minima of free energy.[23,24] They are separated by an energy barrier that is caused by enhanced Coulombic repulsion when double C═C bonds of adjacent molecules are oriented along each other, which is necessary for covalent bonding. The face-centered cubic structure of pristine crystalline fullerene at room temperature is characterized by continuous jumping of the C_{60} molecules between H- and P-orientations, which looks like the rotation of fullerene molecules. The rotation rate decreases with a decreasing temperature since the jumps over the barrier have a thermally activated character. Thereby, the transition of the orientation ordering to the simple cubic phase occurs at 249 K when the rotation of molecules is stopped, and they form the so-called "orientational glass".[23−26] The rate of the photo-induced polymerization at fixed conditions of laser power and beam focusing increases with temperature due to an increase in the rotation rate of C_{60} molecules. The temperature dependence of the photopolymerization rate was studied in pristine C_{60}, as well as in the molecular complexes $\{Pt(dbdtc)_2\}{\cdot}C_{60}$ and $\{Pt(nPr_2dtc)_2\}{\cdot}(C_{60})_2$. In this way, the activation energies of photopolymerization were determined for the first time, which, in fact, are the activation energy of C_{60} cage rotations.[27]

In this letter, we present the results of high-pressure Raman and XRD studies of the $[\{Zn(Et_2dtc)\}_2{\cdot}DABCO]{\cdot}C_{60}{\cdot}(DABCO)_2$ fullerene complex. The Raman spectra measured with a green laser with an excitation of 532 nm show the softening and splitting of the A_g (1) and A_g (2) phonon modes of the fullerene molecules near 2 GPa caused by the formation of covalent bonds between them. At the same time, the pressure dependence of the lattice parameters is smooth and monotonous in the pressure range under study of up to 2.6 GPa, as well as the pressure dependence of the cell volume, which is well described by the Murnaghan equation of state with parameters K_0 = 10.67 GPa and K' = 6.96. There are no signs of polymerization because the smallest distance between the fullerene molecules at 2.6 GPa is 9.6 Å. This exceeds analogous distances of 9.26, 9.2, and 9.09 Å in linear orthorhombic, planar rhombohedral, and planar tetragonal polymers, respectively.[17] More detailed XRD analysis confirmed the absence of covalent bonds between adjacent fullerene molecules. The Raman spectra taken with a poorly absorbed near-infrared laser show the smooth pressure behavior of phonon modes without indications of covalent bonding. The data obtained give evidence of photopolymerization in the fullerene layers that does not take place under ambient conditions and appears at elevated pressure. To clarify the occurrence of photopolymerization at high pressure, we studied the kinetics of photopolymer formation in a temperature region of 266−358 K at three different pressures of 1.05, 1.35, and 1.85 GPa. We found that the activation energy of photopolymerization (related to the rotation of fullerene cages) decreased with pressure from (1.05 ± 0.18) eV at 1.05 GPa to (0.18 ± 0.03) eV at 1.85 GPa, which resulted in rather fast photopolymerization in the fullerene layers of the

https://doi.org/10.1021/acs.jpcc.3c06997
J. Phys. Chem. C 2024, 128, 597−604

$[\{Zn(Et_2dtc)\}_2{\cdot}DABCO]{\cdot}C_{60}{\cdot}(DABCO)_2$ complex at room temperature near 2 GPa.

2. EXPERIMENTAL DETAILS

The samples of the $[\{Zn(Et_2dtc)\}_2{\cdot}DABCO]{\cdot}C_{60}{\cdot}(DABCO)_2$ complex were synthesized by evaporation of a solution containing fullerene acceptors and DABCO donors by the method described in.[28] The structural data were obtained for the high-quality single crystals at ambient and elevated pressures using a four-circle Oxford Diffraction Gemini-R diffractometer equipped with a two-dimensional AtlasS2 CCD (Mo $K\alpha_1$ λ = 0.71073 Å, graphite monochromator, ω-scan) and diamond anvil cell (DAC) with Boehler type Ia diamond anvils. The XRD data showed that the $[\{Zn(Et_2dtc)\}_2{\cdot}DABCO]{\cdot}C_{60}{\cdot}(DABCO)_2$ complex acquired an orthorhombic structure, space group *Pbam* with unit cell parameters a = 10.4349 Å, b = 17.0992 Å, c = 21.1554 Å, and V = 3774.73 Å^3. In the fullerene layers, each C_{60} molecule was surrounded by six neighbors, with the shortest distances between the centers of the fullerene molecules being 10.0158 (four neighbors) and 10.4349 Å (two neighbors). No C−C bonds were found between the fullerene molecules at ambient conditions, and, therefore, the molecules in the fullerene layers were in a monomeric state. The Raman spectra were recorded in the backscattering geometry using an Acton SpectraPro-2500i spectrograph with a green laser of 532 nm and a LabRam HR micro-Raman setup with a near-infrared laser of 785 nm, both equipped with Peltier-cooled CCD detectors. The laser beam was focused on the sample by a 50× objective with laser power before the DAC of 150 μW for the 785 nm laser and 250 μW for the 532 nm laser. The Raman measurements at high pressure were carried out using a Mao-Bell type DAC, while the 4:1 methanol/ethanol mixture was used as a pressure-transmitting medium, and the ruby fluorescence technique was used for pressure calibration.[29] For measurements at high pressure and temperatures in a range of 170−360 K, a self-made compact cylindrical DAC with a diameter/height of about 39 mm was used, which was compatible with a nitrogen cryostat equipped with a temperature controller, and a resistive heat exchanger provided temperature control with an accuracy of ±0.4 K similar to that described earlier in.[30] The DAC was placed into a cylindrical cavity inside the heat exchanger, which ensured good thermal contact with the DAC, while the pressure was set at room temperature with subsequent control when the required temperature was reached.

3. RESULTS AND DISCUSSION

Figure 1 depicts the Raman spectra of the $[\{Zn(Et_2dtc)\}_2{\cdot}DABCO]{\cdot}C_{60}{\cdot}(DABCO)_2$ complex at room temperature and various pressures of up to ∼5 GPa recorded with a green laser of 532 nm (left panel) and a near-infrared laser of 785 nm (central panel). The spectra in the left panel were taken at a laser power of ∼250 μW and exposure time of up to 1 h, whereas in the central panel, the laser power was ∼150 μW, and the exposure time was about the same. The Raman measurements in every case were performed consequently at the same fixed site of the sample for each pressure. The phonon bands in the Raman spectra are related to the A_g and H_g modes of the fullerene molecule due to the dominant contribution of C_{60} in the Raman scattering cross-section of the fullerene complexes with molecular donors.[31] The spectra at ambient conditions are identical in the left and central panels; the phonon bands in both panels demonstrate a positive pressure shift typical of crystals with a van der Waals intermolecular interaction. The difference in the pressure behavior of the Raman spectra appears at pressures above 2 GPa when the phonon bands in the left panel split and broaden, whereas the spectra in the central panel do not show noticeable changes. The right panel in Figure 1 illustrates the pressure dependence of the A_g (2) and A_g (1) phonon mode frequencies. The Raman data obtained with the green laser (solid circles) show a peculiarity near ∼2 GPa, whereas those obtained with the near-infrared laser (solid squares) demonstrate a smooth linear behavior. At pressures below 2 GPa, the data taken with the green and infrared lasers completely match their growing linear behavior. At higher pressure, the data taken with the green laser show sublinear pressure behavior of the A_g (1) mode, while the A_g (2) mode frequency shows a plateau between 2 and 3 GPa and then continues to grow linearly up to ∼8 GPa. The A_g (2) mode frequencies at P < 2 GPa obtained with the green laser and those obtained with the near-infrared laser up to 8 GPa are well described by the linear dependence $\Omega = 1467.8 + 5.5 \times P$ with a pressure coefficient of 5.5 cm^{-1}/GPa and zero pressure frequency of 1467.8 cm^{-1} characteristic of the C_{60} monomer. The data taken with the green laser at pressures between 3 and 8 GPa are also well described by the linear dependence $\Omega = 1461.7 + 5.3 \times P$ with zero pressure value of Ω_0 = 1461.7 cm^{-1}. This value was obtained from extrapolation of the linear dependence to ambient pressure and coincides with the A_g (2) mode frequency of the fullerene dimers C_{120}, which indicates the formation of fullerene dimers under irradiation with a green laser. A similar transformation of the intensity of the A_g (2) PP-mode observed earlier under green laser irradiation in the fullerene complex $\{Cd(dedtc)_2\}_2{\cdot}C_{60}$ was associated with pressure-assisted photoinduced polymerization.[13] The absence of signs of photopolymerization up to 8 GPa in the Raman spectra taken with the near-infrared laser in contrast to those taken with the green laser is related to 10^4 stronger light absorption at 532 nm than that at 785 nm.[32] Thus, photopolymerization under the 785 nm laser is suppressed due to a small number of broken double C═C bonds caused by light absorption, which are insufficient for an effective [2 + 2] cycloaddition reaction. Interestingly, at a pressure of >10 GPa, the Raman spectra taken with the near-infrared laser show weak signs of photoinduced polymerization. This is due to a large red-shift of the C_{60} absorption spectrum that leads to an essential increase in the laser absorption at 785 nm and more intensive breaking of double C═C bonds.[32]

To determine whether the formation of covalent bonds between neighboring fullerene molecules is associated with a dramatic decrease in the distances between fullerene molecules at P > 2 GPa, we performed the XRD measurements at high pressure. Figure 2 depicts the pressure dependence of the lattice parameters of the $[\{Znd(Et_2dtc)\}_2{\cdot}DABCO]{\cdot}C_{60}{\cdot}(DABCO)_2$ complex at pressures of up to 2.6 GPa. The left inset on the bottom of Figure 2 shows the arrangement of the donor and acceptor molecules in the lattice cell at ambient pressure in view along the a-axes, while the right inset shows the arrangement of the C_{60} molecules within the fullerene layers. The open circles in Figure 2 illustrate the pressure dependence of the lattice volume V/V_0, the open squares demonstrate the pressure dependence of the lattice parameter C/C_0 (perpendicular to the molecular layers), and the pentagons denote the pressure dependence of the shortest

https://doi.org/10.1021/acs.jpcc.3c06997
J. Phys. Chem. C 2024, 128, 597−604

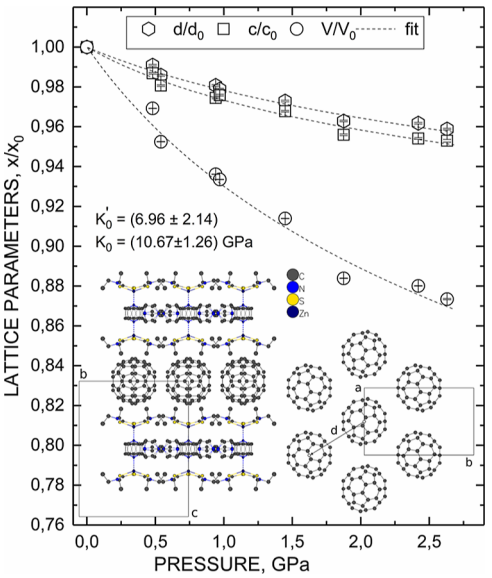

Figure 2. Parameters of the $[\{Zn(Et_2dtc)\}_2 \cdot DABCO] \cdot C_{60} \cdot (DABCO)_2$ crystal lattice versus pressure. Circles—the cell volume V/V_0, squares—parameter c/c_0, and pentagons—the shortest distance between the fullerene molecules d/d_0. Left inset—lattice cell in view along the *a*-axes, and the right inset—lattice cell in view along the *c*-axes.

distance between the fullerene molecules d/d_0, where $d = 1/2(a^2 + b^2)^{1/2}$. The dotted lines are the fits of the experimental data by the Murnaghan equation of state

$$(V/V_0)^{-K'} = \{1 + P \cdot (K'/K_0)\} \quad (1)$$

where $K_0 = (10.67 \pm 1.26)$ GPa is the bulk modulus and $K' = (6.96 \pm 2.14)$ is its derivative, which are close to those of the fullerene crystal in a simple cubic phase.[33] The small value of the bulk modulus and the large value of its derivative are typical for molecular crystals that characterize their high compressibility associated with weak van der Waals intermolecular interaction. The compressibility along the *ab* axes within the molecular layers is smaller than that in a perpendicular direction along the *C* axes due to the layered structure of the molecular complexes. The XRD data show a smooth and monotonous pressure dependence of the lattice parameters without any indication of a phase transition in the pressure region under investigation. The smallest distance between the centers of the fullerene molecules at the highest pressure under study of 2.6 GPa is 9.6 Å. Taking into account that this distance in crystalline C_{60} polymers is 9.26 Å in linear orthorhombic, 9.2 Å in planar rhombohedral, and 9.09 Å in planar tetragonal polymer,[17] it is obvious that no covalent bonds between molecules in the fullerene layers may be formed at 2.6 GPa. This conclusion is confirmed by the detailed XRD analysis that specifies the absence of covalent bonds between adjacent fullerene molecules. The calculations based on the compressibility data show that the covalent bonding in the fullerene layers may be possible at $P > 15$ GPa when the shortest interfullerene distances are close to those typical for intercage distances in fullerene polymers.[16,17]

To confirm that the observed changes between 2 and 3 GPa in the Raman spectra of $[\{Znd(Et_2dtc)\}_2 \cdot DABCO] \cdot C_{60} \cdot (DABCO)_2$ are caused by photopolymerization in the fullerene layers, we examined in detail the evolution of the A_g (2) PP-mode under conditions of long-term laser irradiation at various pressures. The left panel in Figure 3 shows the evolution of the PP-mode in a series of Raman spectra recorded from the same site of the sample at 0.55 GPa, laser power of 250 μW, and λ_{exc} = 532 nm every 10 min. The spectra do not demonstrate changes with an increase in the laser exposure time; thereby, no signs of covalent interfullerene bonding are observed. The central panel depicts the evolution of the Raman spectra recorded at a higher pressure of 1.85 GPa and similar conditions from a new site of the sample. The spectra are gradually transformed with an increase in the laser exposure

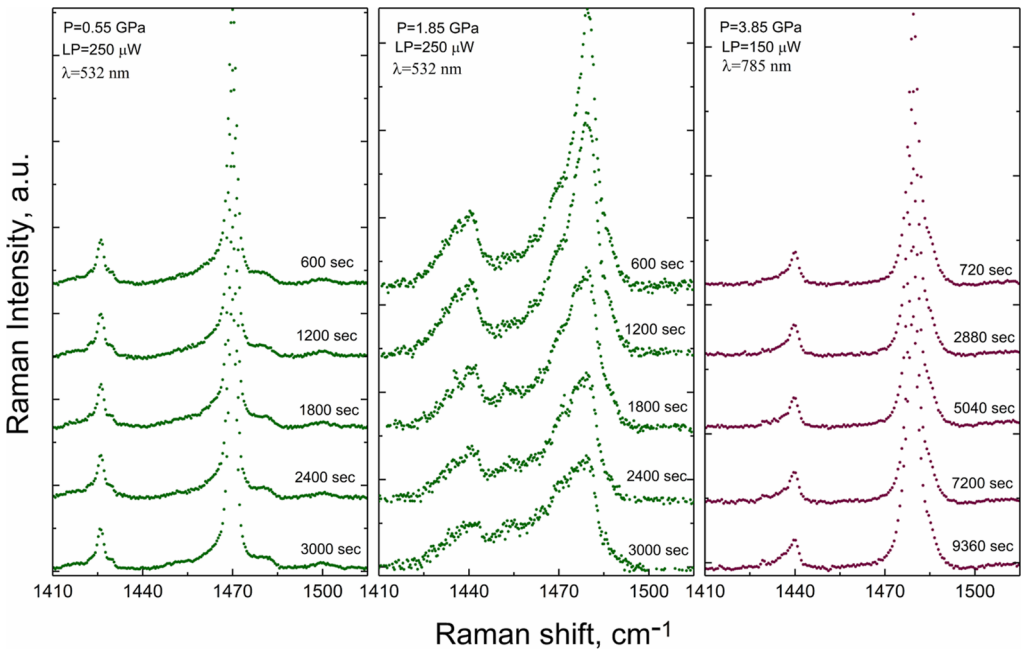

Figure 3. Raman spectra recorded near the A_g (2) PP-mode: left panel—P = 0.55 GPa, central panel—P = 1.85 GPa, λ_{exc} = 532 nm, 250 μW, exposure 10 min. Right panel—P = 3.85 GPa, λ_{exc} = 785 nm, 150 μW, exposure 12 min.

https://doi.org/10.1021/acs.jpcc.3c06997
J. Phys. Chem. C 2024, 128, 597−604

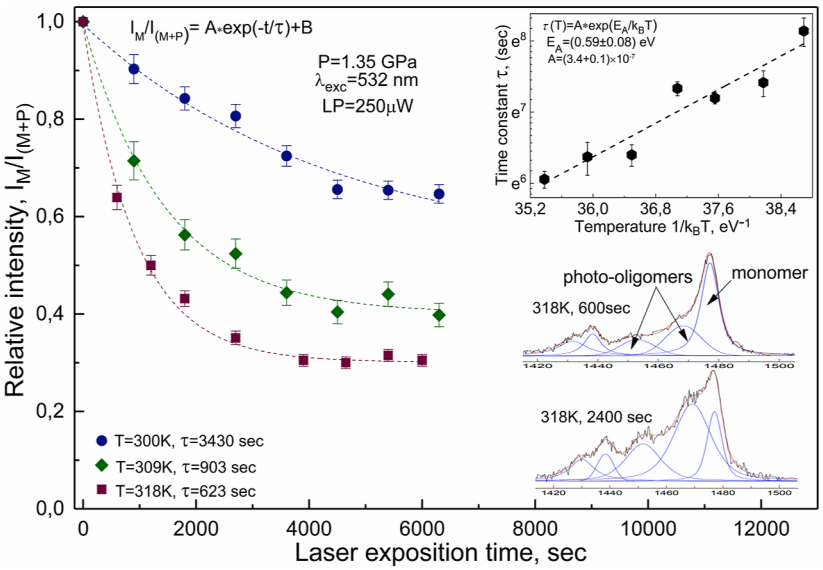

Figure 4. Intensity of the A_g (2) mode monomer with respect to the total intensity of the A_g (2) mode, $I_M/I_{(M+P)}$, versus exposure time. Circles—27 °C, rhombus—36 °C, squares—45 °C, and dashed line—exponential decay fit. Bottom inset: variation of the A_g (2) mode at 1.35 GPa and 45 °C, irradiation 10 and 40 min. Top inset: temperature dependence of the exponential decay time constant, hexagons—experiment, dotted line—linear fit.

time. The main changes are associated with the emergence and growth in intensity of new components near the A_g (2) PP-mode with lower frequencies related to the photo-oligomers of C_{60} similar to those observed in the experiments on fullerene photopolymerization.[3,11,13,15] The right panel in Figure 3 shows the Raman spectra recorded in the same region of the A_g (2) PP-mode at 3.85 GPa with the near-infrared laser of 785 nm every 12 min. These spectra also do not show any changes that may be associated with photopolymerization since it is suppressed due to very small laser light absorption. The characteristic changes in the Raman spectra taken with the green laser at 1.85 GPa are undoubtedly caused by photopolymerization within the laser spot. Thus, the most interesting feature in these experiments is the absence of photopolymerization under ambient conditions and its emergence at elevated pressure, which requires additional study to clarify its nature.

Photopolymerization at ambient conditions in pristine C_{60} and some molecular complexes of fullerene has a thermal activation character.[27] The activation energy of photopolymerization is, in fact, an energy barrier between the H- and P-orientations of the fullerene molecules.[23] The suppression of photopolymerization at room temperature and low pressure in the $[\{Znd(Et_2dtc)\}_2{\cdot}DABCO]{\cdot}C_{60}{\cdot}(DABCO)_2$ complex may be related to a rather high activation energy of C_{60} rotations under ambient conditions. In this case, an increase in the sample temperature may stimulate the rotation of molecules, which results in the emergence of photopolymerization. One should take into account that all fullerene polymers are unstable at elevated temperature and decompose to a monomeric state even under moderate heating.[10,34−40] For example, HPHT 1D-polymers decompose at ∼271 °C, whereas 2D-polymers decompose at ∼284 °C.[34,38] The dimers C_{120} synthesized by a solid-state mechanochemical reaction of C_{60} with potassium cyanide and HPHT dimers transform into monomers at ∼162 and ∼180 °C, respectively.[37,39] As regards photoinduced dimers in pristine C_{60}, they are also stable up to ∼180 °C,[40] while photo-oligomers in the molecular complexes of fullerene are less stable and decompose at a lower temperature of about 130 °C.[10] Thus, to stimulate photopolymerization in fullerene complexes, heating should be carried out carefully to avoid the decomposition of newly formed photo-oligomers at excessive temperature. On the contrary, cooling slows down the rate of photopolymerization when it is initially fast at room temperature, as in the case of the $\{Pt(dbdtc)_2\}{\cdot}C_{60}$ complex or pristine C_{60}.[27] To study the kinetics of photoinduced polymerization, we performed Raman measurements in the $[\{Znd(Et_2dtc)\}_2{\cdot}DABCO]{\cdot}C_{60}{\cdot}(DABCO)_2$ complex at pressures of 1.05, 1.35, and 1.85 GPa and in a temperature range of −7 to +91 °C using the green laser and the homemade DAC equipped with a cryostat/heater. The Raman spectra recorded at 1.05 GPa and 46 °C showed signs of weak photopolymerization 10 min after laser exposure with 250 μW. No signs of photopolymerization were found at similar conditions and ambient temperature; thus, the heating of the sample did lead to the activation of C_{60} rotations, which was necessary for photopolymerization. Figure 4 shows the summary results of Raman measurements with the green laser at a pressure of 1.35 GPa, power of 250 μW, and seven temperatures in a region of 24−55 °C. The Raman spectra were recorded near the A_g (2) PP-mode, which changed significantly; the new red components related to the photo-oligomers of C_{60} appeared and grew in intensity under laser illumination.[13,15] The right inset on the bottom of Figure 4 shows the time evolution of changes in two spectra taken at 1.35 GPa and 45 °C at a laser exposure time of 10 and 40 min. The decomposition of the spectra using the Voigt contour and the calculations of component intensities confirmed a decrease in the primary intensity of the A_g (2) PP-mode associated with the C_{60} monomer and an increase in the intensities of two newly appeared bands related to the photo-oligomers. The relative intensity of the monomeric A_g (2) PP-mode with respect to the total intensity of all modes including the photo-oligomers, $I_M/I_{(M+P)}$, as a function of laser exposure time is shown in the left part of Figure 4. The solid circles, rhombus, and squares show this dependence at 27, 36, and 45 °C,

https://doi.org/10.1021/acs.jpcc.3c06997
J. Phys. Chem. C 2024, 128, 597−604

respectively. The dashed line is the approximation of the experimental data by the exponential decay function

$$I_M/I_{(M+P)} = A\cdot\exp(-t/\tau) + B \quad (2)$$

where τ is the exponential decay time constants, and A and B are the fitting constants. The exponential decay time constant decreased from 3430 s at 27 °C to 623 s at 45 °C, showing the acceleration of photopolymerization with an increase in the temperature. The temperature dependence of the exponential decay time constant τ obtained in a similar way for seven temperatures is shown in the top right inset in Figure 4 in a logarithmic scale as a function of $1/k_BT$. The experimental data are shown with the hexagons, while the dotted line is their best-squares fit. The temperature dependence is well described by the Arrhenius equation

$$\tau(T) = A \times \exp(E_A/k_BT) \quad (3)$$

where $E_A = (0.59 \pm 0.08)$ eV is the activation energy, $A = (3.4 \pm 0.1) \times 10^{-7}$ s is the time constant, k_B is the Boltzmann constant, and T is the temperature. The obtained activation energy is rather high. For example, in the previously studied molecular complex $Pt(nPr_2dtc)_2\}\cdot(C_{60})_2$, which exhibited very fast photopolymerization at ambient conditions, the activation energy was $E_A = (0.13 \pm 0.01)$ eV.[27] For comparison, in some other materials exhibiting photopolymerization at ambient conditions, the activation energy was $E_A = (0.18 \pm 0.01)$ eV in the molecular complex $\{Pt(dbdtc)_2\}\cdot C_{60}$, whereas the highest value $E_A = (0.24 \pm 0.04)$ eV was determined in pristine C_{60}.[27] Interestingly, in the latter case, the activation energy was close to the calculated energy barrier of 0.3 eV between the P- and H- orientations of the C_{60} molecule in solid fullerene.[41]

To study how the activation energy changes with pressure, we examined additionally the kinetics of photopolymerization in the $[\{Zn(Et_2dtc)\}_2\cdot DABCO]\cdot C_{60}\cdot(DABCO)_2$ complex at 1.05 and 1.85 GPa. Generally, an increase in the pressure stimulated photopolymerization, and it became faster. At all pressures under study, photopolymerization had a thermal activation character, and the dependence of the exponential decay time constant on temperature is well described by eq 3. Figure 5 shows the Arrhenius plots at 1.05 GPa with solid squares, 1.35 GPa with solid circles, and 1.85 GPa with a solid rhombus, while the dashed lines are linear fits. The activation energy of photopolymerization gradually decreased with an increase in the pressure from $E_A = (1.09 \pm 0.18)$ eV at 1.05 GPa to $E_A = (0.59 \pm 0.08)$ eV at 1.35 GPa and, finally, to $E_A = (0.18 \pm 0.0.05)$ eV at 1.85 GPa; the appropriate pressure dependence is shown in the right top inset in Figure 5. We believe that the activation energy under ambient conditions was actually higher than that at 1.05 GPa. This may be a case when photopolymerization could not be activated even at too high temperatures since it could reach the limit of stability of photo-oligomers and caused their decomposition. The right bottom inset in Figure 5 illustrates a schematic picture of energy levels in pristine fullerene monomers and dimers. The monomer is shown in the local minimum of energy on the left side of the scheme, while the dimers are shown in the other local minimum on the right side. The difference between the two minima ΔE is related to the binding energy of the dimers, while the energy barrier E_A between them is, in fact, the activation energy of C_{60} rotations. The barrier between the two minima is due to enhanced Coulombic repulsion between molecules oriented toward each other by electron-reach double C═C bonds.

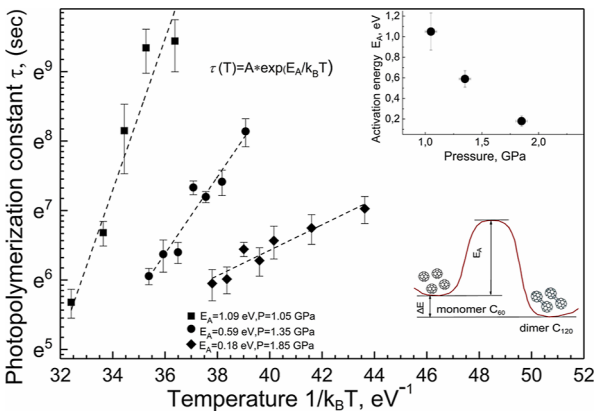

Figure 5. Arrhenius dependence of the exponential decay time constant: squares—1.05 GPa, circles—1.35 GPa, rhombus—1.85 GPa, and dashed line—linear fit. Top inset: activation energy E_A versus pressure. Bottom inset: scheme of energy levels for the monomers and dimers.

To sum up, the experimentally measured activation energy of photopolymerization in the $[\{Zn(Et_2dtc)\}_2\cdot DABCO]\cdot C_{60}\cdot(DABCO)_2$ complex at 1.05 GPa is about 4.5 times higher than that in pristine C_{60}. However, it decreases significantly with the pressure becoming even less than that in pristine C_{60} at 1.85 GPa. The numerical data obtained earlier and in the present work mean that the molecular donor could affect the magnitude of the energy barrier between the P- and H-orientations of fullerene molecules in the molecular complexes. Actually, the energy barriers differ from each other in a number of already studied fullerene complexes, as well as from that in pristine C_{60}.[27] This may be due to specific configurations of the donor molecules used and different overlaps of the HOMO of the molecular donor and the LUMO of the fullerene acceptor, which give rise to charge transfer between them. The most interesting, in our opinion, is that the energy barrier gradually decreases with pressure as it was found in the $[\{Zn(Et_2dtc)\}_2\cdot DABCO]\cdot C_{60}\cdot(DABCO)_2$ complex and another well-known fullerene complex with ferrocene $C_{60}\cdot\{Fe(C_5H_5)_2\}_2$ (unpublished experimental data). At first glance, this looks paradoxical because the van der Waals repulsion increases at high pressure with decreasing intermolecular distances. The energy barrier between the P- and H-orientations caused by Coulombic repulsion changes at high pressure due to the transfer of the charge and its distribution on the fullerene molecule cage. This behavior was observed earlier in the fullerene complex with ferrocene $C_{60}\cdot\{Fe(C_5H_5)_2\}_2$, where the asymmetric charge transfer resulted in a redistribution of charges on the fullerene molecule cage intensified with increasing pressure.[42] The variety of molecular orbitals and the changes in the overlap of the donor and acceptor HOMO/LUMO orbitals at high pressure lead to the different activation energy of photo-induced polymerization of various complexes, which changes additionally at high pressure.

4. CONCLUSIONS

The Raman spectra of the $[\{Zn(Et_2dtc)\}_2\cdot DABCO]\cdot C_{60}\cdot(DABCO)_2$ complex recorded at high pressure when using a highly absorbable green laser showed the splitting of H_g modes and softening of the A_g modes of fullerene molecules near 2 GPa, indicating covalent bonding. The pressure dependence of the lattice parameters was smooth and monotonous, and the

https://doi.org/10.1021/acs.jpcc.3c06997
J. Phys. Chem. C 2024, 128, 597−604

shortest interfullerene distance at the highest pressure of 2.6 GPa significantly exceeded those in fullerene HPHT polymers. The detailed XRD analysis did not show covalent bonding in the pressure range under study. The changes in the Raman spectra near 2 GPa resulted from photoinduced polymerization in the fullerene layers under green laser irradiation. The polymerization was suppressed when using a less absorbable near-infrared laser because of the amount of broken double C═C bonds insufficient to activate the [2 + 2] cycloaddition reaction. The thermally activated photoinduced polymerization shoved the activation energy that decreased with pressure from $E_A = (1.09 \pm 0.18)$ eV at 1.05 GPa to $E_A = (0.59 \pm 0.08)$ eV at 1.35 GPa and, finally, to $E_A = (0.18 \pm 0.0.05)$ eV at 1.85 GPa. The barrier between the H- and P-orientations of fullerene molecules depended on the molecular donor and was different for pristine fullerene and its complexes with different donors. The barrier in the $[\{Zn(Et_2dtc)\}_2{\cdot}DABCO]{\cdot}C_{60}{\cdot}(DABCO)_2$ complex, which was initially high under ambient conditions, decreased with pressure due to the changes in the overlap of the donor and acceptor molecular orbitals caused by partial charge transfer and redistribution of charges on the fullerene cage.

AUTHOR INFORMATION

Corresponding Author

Konstantin P. Meletov − *Osipyan Institute of Solid State Physics RAS, Chernogolovka, Moscow Region 142432, Russia;* orcid.org/0009-0002-0261-5634; Email: mele@issp.ac.ru

Authors

Alexey V. Kuzmin − *Osipyan Institute of Solid State Physics RAS, Chernogolovka, Moscow Region 142432, Russia;* orcid.org/0000-0001-8218-4058

Maxim A. Faraonov − *Institute of Problems of Chemical Physics RAS, Chernogolovka, Moscow Region 142432, Russia;* orcid.org/0000-0003-0805-601X

Complete contact information is available at: https://pubs.acs.org/10.1021/acs.jpcc.3c06997

Notes

The authors declare no competing financial interest.

ACKNOWLEDGMENTS

Structural analysis of the $[\{Zn(Et_2dtc)\}_2{\cdot}DABCO]{\cdot}C_{60}{\cdot}(DABCO)_2$ complex crystals and Raman measurements were carried out within the research project of ISSP RAS funded by the Ministry of Science and Higher Education of the Russian Federation (registration number AAAA-A17-117121120049-3). The single crystals were obtained with the support of the Ministry of Science and Higher Education of the Russian Federation (registration number AAAA-A19-119092390079-8). K.P.M. is thankful to the Aristotle University of Thessaloniki, Greece, for the access to the near-infrared Raman instrumentation.

REFERENCES

(1) Cui, W.; Yao, M.; Liu, D.; Li, Q.; Liu, R.; Zou, B.; Cui, T.; Liu, B. Reversible polymerization in doped fullerides under pressure: the case of $C_{60}{\cdot}\{Fe(C_5H_5)_2\}_2$. *J. Phys. Chem. B* **2012**, *116*, 2643−2650.

(2) Meletov, K. P.; Konarev, D. V. Raman study of the pressure-induced phase transitions in the molecular donor-acceptor complex $\{Pt(dbdtc)_2\}{\cdot}C_{60}$. *Chem. Phys. Lett.* **2012**, *553*, 21−25.

(3) Kato, K.; Murata, H.; Gonnokami, H.; Tachibana, M. Polymerization in ferrocene-doped C_{60} nanosheets under high pressure and light irradiation. *Carbon* **2016**, *107*, 622−628.

(4) Cui, W.; Sundqvist, B.; Sun, Sh.; Yao, M.; Liu, B. High pressure and high temperature induced polymerization of doped C_{60} materials. *Carbon* **2016**, *109*, 269−275.

(5) Sun, S.; Cui, W.; Wang, S.; Liu, B. Investigation of the polymerization mechanism of ferrocene doped C_{60} under high pressure and high temperature. *Sci. Rep.* **2017**, *7*, 10809.

(6) Cui, W.; Sun, Sh.; Sundqvist, B.; Wang, Sh.; Liu, B. Pressure induced metastable polymerization in doped C_{60} materials. *Carbon* **2017**, *115*, 740−745.

(7) Wang, L. Solvated fullerenes, a new class of carbon materials suitable for high-pressure studies: A review. *Phys. Chem. Solids* **2015**, *84*, 85−95.

(8) Pei, C.; Feng, M.; Yang, Zh.; Yao, M.; Yuan, Y.; Li, X.; Hu, B.; Shen, M.; Chen, B.; Sundqvist, B.; et al. Quasi 3D polymerization in C_{60} bilayers in a fullerene solvate. *Carbon* **2017**, *124*, 499−505.

(9) Meletov, K. P.; Kuzmin, A. V.; Khasanov, S. S.; Konarev, D. V. X-ray difraction and Raman study of pressure-assisted photo-polymerization in the ferrocene-doped C_{60} crystals. *J. Polym. Res.* **2021**, *28*, 38.

(10) Meletov, K. P.; Velkos, G.; Arvanitidis, J.; Christofilos, D.; Kourouklis, G. A. Raman study of the photopolymer formation in the $\{Pt(dbdtc)_2\}{\cdot}C_{60}$ fullerene complex and the decomposition kinetics of the photo-oligomers. *Chem. Phys. Lett.* **2017**, *681*, 124−129.

(11) Meletov, K. P. Photopolymerization in the fullerene layers of the molecular donor-acceptor complex $\{Pt(nPr_2dtc)_2\}{\cdot}(C_{60})_2$. *Phys. Solid State* **2018**, *60*, 2103−2108.

(12) Rao, A. M.; Zhou, P.; Wang, K.-A.; Hager, G. T.; Holden, J. M.; Wang, Y.; Lee, W.-T.; Bi, X.-X.; Eklund, P. C.; Cornett, D. S.; et al. Photoinduced polymerization of solid C_{60} films. *Science* **1993**, *259*, 955−957.

(13) Meletov, K. P.; Konarev, D. V.; Tolstikova, A. O. Phase transitions and photoinduced transformations at high pressure in the molecular donor-acceptor fullerene complex $\{Cd(dedtc)_2\}_2{\cdot}C_{60}$. *JETP* **2015**, *120*, 989−997.

(14) Pusztai, T.; Oszlanyi, G.; Faigel, G.; Kamaras, K.; Granasy, L.; Pekker, S. Bulk structure of phototransformed C_{60}. *Solid State Commun.* **1999**, *111*, 595−599.

(15) Karachevtsev, V. A.; Mateichenko, P. V.; Nedbailo, N. Y.; Peschanskii, A. V.; Plokhotnichenko, A. M.; Vovk, O. M.; Zubarev, E. N.; Rao, A. M. Effective photopolymerization of C_{60} films under simultaneous deposition and UV light irradiation: Spectroscopy and morphology study. *Carbon* **2004**, *42*, 2091−2098.

(16) Iwasa, Y.; Arima, T.; Fleming, R. M.; Siegrist, T.; Zhou, O.; Haddon, R. C.; Rothberg, L. J.; Lyons, K. B.; Carter, H. L.; Hebard, A. F.; et al. New phases of C_{60} synthesized at high pressure. *Science* **1994**, *264*, 1570−1572.

(17) Nunez-Regueiro, M.; Marques, L.; Hodeau, J.-L.; Bethoux, O.; Perroux, M. Polymerized fullerite structures. *Phys. Rev. Lett.* **1995**, *74*, 278−281.

(18) Zhou, P.; Dong, Z. H.; Rao, A. M.; Eklund, P. Reaction mechanism for photopolymerization of solid fullerene C_{60}. *Chem. Phys. Lett.* **1993**, *211*, 337−340.

(19) Rao, A. M.; Eklund, P. C.; Hodeau, J.-L.; Marques, L.; Nunez-Regueiro, M. Infrared and Raman studies of pressure-polymerized C_{60}. *Phys. Rev. B: Condens. Matter Mater. Phys.* **1997**, *55*, 4766−4773.

(20) Wågberg, T.; Jacobsson, P.; Sundqvist, B. Comparative Raman study of the photopolymerized and pressure-polymerized C_{60} films. *Phys. Rev. B: Condens. Matter Mater. Phys.* **1999**, *60*, 4535−4538.

(21) Davydov, V. A.; Kashevarova, L. S.; Rakhmanina, A. V.; Senyavin, V. M.; Ceolin, R.; Szwarc, H.; Allouchi, H.; Agafonov, V. Spectroscopic study of pressure polymerized phases of C_{60}. *Phys. Rev. B: Condens. Matter Mater. Phys.* **2000**, *61*, 11936−11945.

(22) Winter, J.; Kuzmany, H.; Soldatov, A.; Persson, P.-A.; Jacobsson, J.; Sundqvist, B. Charge transfer in alkali-doped polymeric fullerene. *Phys. Rev. B: Condens. Matter Mater. Phys.* **1996**, *54*, 17486.

(23) David, W. I. F.; Ibberson, R. M.; Dennis, T. J. S.; Hare, J. P.; Prassides, K. Structural phase transitions in the fullerene C_{60}. *Europhys. Lett.* **1992**, *18*, 219−225.
(24) David, W. I. F.; Ibberson, R. M. High-pressure, low-temperature structural studies of orientationally ordered C_{60}. *J. Phys.: Condens. Matter* **1993**, *5*, 7923−7928.
(25) Heiney, P. A.; Fischer, J. E.; McGhie, A. R.; Romanow, W. J.; Denenstein, A. M.; McCauley Jr, J. P.; Smith, A. B.; Cox, D. E. Orientational ordering transition in solid C_{60}. *Phys. Rev. Lett.* **1991**, *66*, 2911−2914.
(26) Gugenberger, F.; Heid, R.; Meingast, C.; Adelmann, P.; Braun, M.; Wühl, H.; Haluska, M.; Kuzmany, H. Glass transition in single-crystal C_{60} studied by high-resolution dilatometry. *Phys. Rev. Lett.* **1992**, *69*, 3774−3777.
(27) Meletov, K. P. The photopolymerization rate and activation energy of C_{60} rotations in fullerene and its molecular complexes. *Fullerenes Nanotubes Carbon Nanostruct.* **2020**, *28*, 93−96.
(28) Konarev, D. V.; Khasanov, S. S.; Lopatin, D. V.; Rodaev, V. V.; Lyubovskaya, R. N. Fullerene complexes with divalent metal dithiocarbamates: structures, magnetic properties, and photoconductivity. *Russ. Chem. Bull., Int. Ed.* **2007**, *56*, 2145−2161.
(29) Jayaraman, A. Ultrahigh pressures. *Rev. Sci. Instrum.* **1986**, *57*, 1013−1031.
(30) Meletov, K. P. A nitrogen cryostat with adjustable temperature and cold loading of samples for the measurement of optical spectra. *Instrum. Exp. Tech.* **2020**, *63*, 291−293.
(31) Meletov, K. P. Phase Transitions at High Pressure in the Fullerene C_{60} Molecular Donor−Acceptor Complex $\{Hg(dedtc)_2\}_2 \cdot C_{60}$. *Phys. Solid State* **2014**, *56*, 1689−1695.
(32) Meletov, K. P.; Dolganov, V. K.; Zharikov, O. V.; Kremenskaya, I. N.; Ossipyan, Y. A.; Yu, A. Absorption Spectra of Crystalline Fullerite C_{60} at Pressures up to 19 GPa. *J. Phys. I* **1992**, *2*, 2097−2105.
(33) Lundin, A.; Sundqvist, B. Compressibility of C_{60} in the temperature range 150−335 K up to a pressure of 1 GPa. *Phys. Rev. B: Condens. Matter Mater. Phys.* **1996**, *53*, 8329−8336.
(34) Iwasa, Y.; Tanoue, K.; Mitani, T.; Yagi, T. Energetics of polymerized fullerites. *Phys. Rev. B: Condens. Matter Mater. Phys.* **1998**, *58*, 16374−16377.
(35) Korobov, M. V.; Senyavin, V. M.; Bogachev, A. G.; Stukalin, E. B.; Davydov, V. A.; Kashevarova, L. S.; Rakhmanina, A. V.; Agafonov, V.; Szwarc, A. Phase transformations in pressure polymerized C_{60}. *Chem. Phys. Lett.* **2003**, *381*, 410−415.
(36) Nagel, P.; Pasler, V.; Lebedkin, S.; Soldatov, A.; Meingast, C.; Sundqvist, B.; Persson, P.-A.; Tanaka, T.; Komatsu, K.; Buga, S.; et al. C_{60} one- and two-dimensional polymers, dimers, and hard fullerite: Thermal expansion, anharmonicity, and kinetics of depolymerization. *Phys. Rev. B: Condens. Matter Mater. Phys.* **1999**, *60*, 16920−16927.
(37) Wang, G.-W.; Komatsu, K.; Murata, Y.; Shiro, M. Synthesis and X-ray structure of dumb-bell-shaped C_{120}. *Nature* **1997**, *387*, 583−586.
(38) Meletov, K. P.; Arvanitidis, J.; Christofilos, D.; Kourouklis, G. A.; Iwasa, Y.; Yamanaka, S. Temperature-induced decomposition of the two dimensional rhombohedral polymer of C_{60}: Raman study of the intermediate state. *Carbon* **2010**, *48*, 2974−2979.
(39) Meletov, K. P.; Arvanitidis, J.; Christofilos, D.; Kourouklis, G. A.; Davydov, V. A. Raman study of the temperature-induced decomposition of the fullerene dimers C_{120}. *Chem. Phys. Lett.* **2016**, *654*, 81−85.
(40) Wang, Y.; Holden, J. M.; Bi, X.-X.; Eklund, P. C. Thermal decomposition of polymeric C_{60}. *Chem. Phys. Lett.* **1994**, *217*, 413−417.
(41) Burgos, E.; Halac, E.; Bonadeo, H. Intermolecular Forces and Phase Transitions in Solid C_{60}. *Phys. Rev. B: Condens. Matter Mater. Phys.* **1994**, *49*, 15544−15549.
(42) Kuzmin, A. V.; Meletov, K. P.; Khasanov, S. S.; Faraonov, M. A. Pressure-induced donor-acceptor charge transfer in a fullerene molecular complex with ferrocene. *J. Phys. Chem. C* **2021**, *125*, 16576−16582.

https://doi.org/10.1021/acs.jpcc.3c06997
J. Phys. Chem. C 2024, 128, 597−604